Reversible Pharmacokinetic Profiles of Canrenoic Acid and Its Biotransformed Product, Canrenone in the Rat

Shozo ASADA,* Tomoko OHTAWA and Hiroko NAKAE

Kobe Women's College of Pharmacy, Motoyamakita-machi, Higashinada-ku, Kobe 658, Japan. *Received June 22, 1989*

Pharmacokinetic profiles of canrenoic acid (CRA) and canrenone (CR), the reversible metabolite of CRA, were studied in the rat after intraportal (pv) administration in comparison with those after intravenous (iv) administration using an interconversion model. In the clearances for the irreversible loss, CL_{20} of CR was larger than CL_{10} of CRA. Nevertheless, the real plasma clearance of CR was less than that of CRA. The distribution volume V_1 of CRA was almost close to the real distribution volume $V_{ss,real,D}$ of CRA at the steady state. The hepatic available fraction of CRA, F_{H1} and sequential hepatic available fraction of generated metabolite, F_{H2}, were estimated.

Simultaneous computer multi-line fitting of plasma concentration–time data was carried out and the adequacy of pharmacokinetic parameters in this model was tested using the iterative nonlinear least-squares regression program, MULTI.

Keywords reversible pharmacokinetics; canrenoic acid; canrenone; portal vein administration; first-pass metabolism; interconversion model; multi-line fitting

Potassium canrenoate [Soldactone®, potassium 17β-hydroxy-3-oxo-17α-pregna-4,6-diene-21-carboxylate], (CRA-K) is used as a water-soluble steroidal diuretic. It is structurally related to spironolactone [Aldactone®], a useful aldosterone antagonist. Canrenoic acid (CRA), the free form of CRA-K, is found to be in enzymatic equilibrium with canrenone (CR),[1-5] while CRA and CR are chemically rather stable *in vitro* at the pH of plasma.[6] CRA is mainly excreted into urine as its ester glucuronide,[7] but it is presumed[8] that the pharmacological activities of spironolactone and CRA-K may be related to the urinary excretion of CR in man.

The purpose of the study described here was to characterize the reversible pharmacokinetics of the CRA–CR system and to estimate the available fractions of CRA as a prodrug and CR in the rat.

Theoretical

An interconversion model which incorporates a first-pass biotransformation is illustrated in Fig. 1.[9] This model assumes that both the parent drug (D) and its relevant metabolite (M) have linear dispositions and that elimination and interconversion processes are restricted to the respective central compartments.

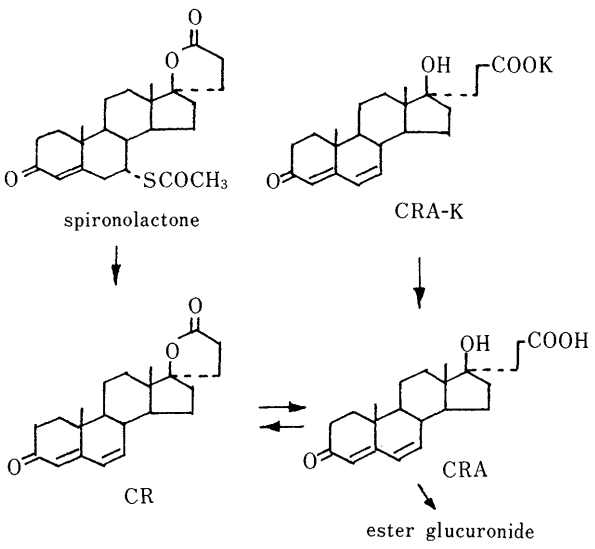

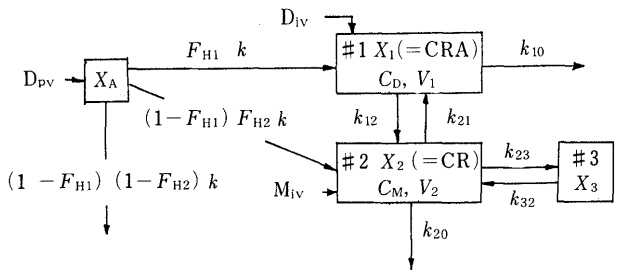

Fig. 1. Linear Interconversion Model with First-Order Input Step Describing the Pharmacokinetics of Canrenoic Acid CRA (D) and Its Metabolite CR (M) in the Rat

See the text for details.

The symbol X_i ($i=1$ to 3) is the amount of drug in the central (#1 and #2) and peripheral (#3) compartments, k, k_{12}, k_{21}, k_{23} and k_{32} are the first-order rate constants describing the drug transfer, and k_{10} and k_{20} are the first-order rate constants describing the drug loss from the compartment. The intravenous (iv) administration of the drug, CRA-K, may be made into compartment #1 of distribution volume V_1 to give a concentration C_D of CRA. Alternatively, administration of CRA-K through the hepatic portal vein (pv) may be made, where X_A is the amount of CRA at the administered site. CRA may be eliminated by clearances CL_{12} ($=k_{12}V_1$) and CL_{10} ($=k_{10}V_1$). The metabolite, CR, administered intravenously occupies a distribution volume V_2 at compartment #2 to give a concentration C_M, and may be eliminated by the clearances CL_{21} ($=k_{21}V_2$) to generate CRA and CL_{20} ($=k_{20}V_2$). Following pv administration of CRA-K, a certain fraction of X_A enters compartment #1 intact (F_{H1}), escaping hepatic biotransformation. A part of the remaining fraction ($1-F_{H1}$) of X_A undergoes first-pass biotransformation entering the systemic circulation (compartment #2) as a metabolite, CR. The F_{H2} indicates the fraction of the generated metabolite CR which enters compartment #2, escaping sequential hepatic biotransformation.[10]

After an iv dose of the drug (D_{iv}), plasma concentration profiles of drug and metabolite can be measured. When the distributional clearances of metabolite between compart-

ments #2 and #3 are proportional in Fig. 1, mass balance considerations indicate that

$$CL_{10}^{D_{iv}} AUC_D^{D_{iv}} + CL_{20}^{D_{iv}} AUC_M^{D_{iv}} = \text{dose}^{D_{iv}} \quad (1)$$

$$CL_{12}^{D_{iv}} AUC_D^{D_{iv}} - (CL_{20}^{D_{iv}} + CL_{21}^{D_{iv}}) AUC_M^{D_{iv}} = 0 \quad (2)$$

Similarly, after an iv dose of the preformed metabolite (M_{iv}), the corresponding expressions are

$$CL_{10}^{M_{iv}} AUC_D^{M_{iv}} + CL_{20}^{M_{iv}} AUC_M^{M_{iv}} = \text{dose}^{M_{iv}} \quad (3)$$

$$(CL_{10}^{M_{iv}} + CL_{12}^{M_{iv}}) AUC_D^{M_{iv}} - CL_{21}^{M_{iv}} AUC_M^{M_{iv}} = 0 \quad (4)$$

where administered drug doses are given in molar unit, AUC_i (i=D and M) indicates the total area under the plasma concentration *vs.* time curve and superscripts represent the route of administration of the drug and the metabolite.

The four fundamental clearances[11] in the reversible drug–metabolite system may be determined by solving Eqs. 1—4. If all clearance terms remain constant between treatments such that

$$\left.\begin{aligned} CL_{10}^{D_{iv}} = CL_{10}^{M_{iv}} = CL_{10}, \quad CL_{12}^{D_{iv}} = CL_{12}^{M_{iv}} = CL_{12} \\ CL_{20}^{D_{iv}} = CL_{20}^{M_{iv}} = CL_{20}, \quad CL_{21}^{D_{iv}} = CL_{21}^{M_{iv}} = CL_{21} \end{aligned}\right\} \quad (5)$$

then the following equations are derived from Eqs. 1 and 3.

$$CL_{10} = \frac{AUC_M^{M_{iv}} \text{dose}^{D_{iv}} - AUC_D^{D_{iv}} \text{dose}^{M_{iv}}}{AUC_D^{D_{iv}} AUC_M^{M_{iv}} - AUC_M^{D_{iv}} AUC_D^{M_{iv}}} \quad (6)$$

and

$$CL_{20} = \frac{AUC_D^{D_{iv}} \text{dose}^{M_{iv}} - AUC_D^{M_{iv}} \text{dose}^{D_{iv}}}{AUC_D^{D_{iv}} AUC_M^{M_{iv}} - AUC_M^{D_{iv}} AUC_D^{M_{iv}}} \quad (7)$$

Subsequently, from Eqs. 2 and 4,

$$CL_{12} = \frac{AUC_M^{D_{iv}} \text{dose}^{M_{iv}}}{AUC_D^{D_{iv}} AUC_M^{M_{iv}} - AUC_M^{D_{iv}} AUC_D^{M_{iv}}} \quad (8)$$

and

$$CL_{21} = \frac{AUC_D^{M_{iv}} \text{dose}^{D_{iv}}}{AUC_D^{D_{iv}} AUC_M^{M_{iv}} - AUC_M^{D_{iv}} AUC_D^{M_{iv}}} \quad (9)$$

A system of first-order linear differential equations with constant coefficients can be written from Fig. 1:

$$dX_A/dt = -[F_{H1} + (1-F_{H1})F_{H2} + (1-F_{H1})(1-F_{H2})]kX_A = -kX_A \quad (10)$$

$$dX_1/dt = F_{H1} kX_A - E_1 X_1 + k_{21} X_2 \quad (11)$$

$$dX_2/dt = (1-F_{H1})F_{H2} kX_A + k_{12} X_1 - E_2 X_2 + k_{32} X_3 \quad (12)$$

$$dX_3/dt = k_{23} X_2 - k_{32} X_3 \quad (13)$$

where E_i (i=1 to 2) is the sum of first-order exit rate constants from each compartment, and the amounts of drug after pv administration are $X_A = \text{dose}^{D_{pv}}$ and $X_1 = X_2 = X_3 = 0$ at the initial time, respectively.

The Laplace transforms[12] of the plasma concentration *vs.* time equation of the drug $\tilde{C}_D(s)$ and its metabolite $\tilde{C}_M(s)$ after pv administration of drug (D_{pv}), for instance, are given by Eqs. 14 and 15.

$$\tilde{C}_D^{D_{pv}}(s) = \frac{\text{dose}^{D_{pv}} k}{V_1} \left[\frac{F_{H1}(s+R)(s+S) + (1-F_{H1})F_{H2} k_{21}(s+k_{32})}{(s+\alpha)(s+\beta)(s+\gamma)(s+k)} \right] \quad (14)$$

$$\tilde{C}_M^{D_{pv}}(s) = \frac{\text{dose}^{D_{pv}} k}{V_2} \left[\frac{F_{H1} k_{12}(s+k_{32}) + (1-F_{H1})F_{H2}(s+\alpha)(s+k_{32})}{(s+\alpha)(s+\beta)(s+\gamma)(s+k)} \right] \quad (15)$$

where α, β, γ, R and S represent the individual rate constants, and s is the Laplace parameter. The following relationships hold:

$$\left.\begin{aligned} E_1 = k_{10} + k_{12} = \alpha \\ E_2 = k_{20} + k_{21} + k_{23} \end{aligned}\right\} \quad (16)$$

$$(s+R)(s+S) = (s+E_2)(s+k_{32}) - k_{23} k_{32} \quad (17)$$

$$RS = k_{32}(k_{20} + k_{21}) \quad (18)$$

$$\beta + \gamma = R + S = E_2 + k_{32} \quad (19)$$

$$\beta\gamma = k_{32}(k_{10}k_{20} + k_{10}k_{21} + k_{12}k_{20})/(k_{10} + k_{12}) \quad (20)$$

$$\text{and } R \text{ or } S = [(\beta+\gamma) \pm \sqrt{(\beta+\gamma)^2 - 4k_{32}(k_{20}+k_{21})}]/2, \quad (\beta > R > S > \gamma) \quad (21)$$

AUC values are given as $AUC = \lim_{s \to 0} \tilde{C}(s)$.[13] The general solutions for AUC's under different administration routes of the drug and preformed metabolite are summarized in Table I (Eqs. 22—27).

Using the AUC values given in Table I, systemic available fractions[14,15] are defined by Eq. 28 for the drug, and by Eq. 29 for its relevant metabolite.

$$F_D = (AUC_D^{D_{pv}}/\text{dose}^{D_{pv}})/(AUC_D^{D_{iv}}/\text{dose}^{D_{iv}}) = 1 - (1-F_{H1})[1 - F_{H2} \cdot f_d] \quad (28)$$

$$F_M = (AUC_M^{D_{pv}}/\text{dose}^{D_{pv}})/(AUC_M^{D_{iv}}/\text{dose}^{D_{iv}}) = 1 + (1-F_{H1})[F_{H2}/f_m - 1] \quad (29)$$

where f_d and f_m are conversion fractions as cited in the experimental section. Then, the available fraction as the sum of both drug and its metabolite is given by Eq. 30.

$$F = \frac{(CL_{10} AUC_D^{D_{pv}} + CL_{20} AUC_M^{D_{pv}})/\text{dose}^{D_{pv}}}{(CL_{10} AUC_D^{D_{iv}} + CL_{20} AUC_M^{D_{iv}})/\text{dose}^{D_{iv}}} = 1 - (1-F_{H1})(1-F_{H2}) \quad (30)$$

Table I. Areas under the Curve of the Drug and Its Metabolite after Intravenous and Portal Vein Administrations[a]

Compound	Route of administration	AUC[b]	Eq.
Drug (CRA-K)	Intraportal	$AUC_D^{D_{pv}} = \text{dose}^{D_{pv}} k_{32}[F_{H1}(k_{20}+k_{21}) + (1-F_{H1})F_{H2}k_{21}]/V_1\alpha\beta\gamma$	22
		$AUC_M^{D_{pv}} = \text{dose}^{D_{pv}} k_{32}[F_{H1}k_{12} + (1-F_{H1})F_{H2}(k_{10}+k_{12})]/V_2\alpha\beta\gamma$	23
	Intravenous	$AUC_D^{D_{iv}} = \text{dose}^{D_{iv}}(k_{20}+k_{21})k_{32}/V_1\alpha\beta\gamma$	24
		$AUC_M^{D_{iv}} = \text{dose}^{D_{iv}} k_{12}k_{32}/V_2\alpha\beta\gamma$	25
Preformed metabolite (CR)	Intravenous	$AUC_M^{M_{iv}} = \text{dose}^{M_{iv}} k_{32}/V_2\beta\gamma$	26
		$AUC_D^{M_{iv}} = \text{dose}^{M_{iv}} k_{21}k_{32}/V_1\alpha\beta\gamma$	27

a) There are the following relationships among the first-order rate constants: $\alpha = k_{10} + k_{12}$, $\beta + \gamma = k_{20} + k_{21} + k_{23} + k_{32}$ and $\beta\gamma = k_{32}[k_{10}k_{20} + k_{10}k_{21} + k_{12}k_{20}]/(k_{10} + k_{12})$. *b*) Superscripts indicate the route of administration of CRA-K (D) and CR (M).

The hepatic available fraction F_{H1} and sequential hepatic available fraction F_{H2} are obtained by solving the simultaneous Eqs. 28 and 29.

Experimental

Meterials CRA-K was purchased from Sigma Chemical Co. (St. Louis, U.S.A.). CR was obtained as follows[16]: after stirring CRA-K (1.0 g) with 2 ml of HCl and 3.6 ml of water in 20 ml of MeOH for 3 h, the white crystals were collected and recrystallized from AcOEt–ether, mp 135—137 °C. Fluorene (FL) as an internal standard for high-performance liquid chromatography (HPLC) and other reagents were of special reagent grade.

Chromatographic Conditions HPLC was carried out using a Shimadzu LC-6A apparatus equipped with a variable-wavelength photometric detector (Shimadzu SPD-6A), column oven (Shimadzu CTO-6A), reversed-phase column (Cosmosil $5C_8$, 0.46 i.d. × 15 cm) and guard column (Cosmosil $10C_8$, 0.46 i.d. × 5 cm). The column was maintained at 35 °C and eluted with 0.5% AcOH–MeCN (4:6, volume ratio) at a flow rate of 0.7 ml/min. The elution was monitored at 285 nm (0.08 AUFS). Retention times were as follows: 4.6 min for CRA, 8.2 min for CR and 15 min for FL (internal standard). Regression lines for calibration were obtained by least-squares analysis of ratios of the peak areas of drug concentration at 0.00025, 0.0005, 0.001, 0.005, 0.01, 0.05 and 0.1 μmol/ml to the peak area of 0.1 μg/ml of FL in rat plasma, bile and urine (Table II).

Animal Experiments Male Wistar rats (Shizuoka Laboratory Animal Center, Hamamatsu, Japan), weighing 250—380 g, were anesthetized with sodium pentobarbital (50 mg/kg, intraperitoneally). The jugular vein, bile fistula or urinary bladder were each cannulated with polyethylene tubing. After the cannulation, a bolus injection of 0.03 mmol/kg of CRA-K or CR was made intravenously (iv) or through the portal vein (pv). After dosing, blood samples were drawn through the cannula at appropriate time intervals and then were centrifuged immediately to separate the plasma. Bile and urine samples were collected through the cannulas during 6 h after drug injection.

Sample Analysis Samples of 200 μl for plasma, bile or urine were added to 200 μl of internal standard solution (100 μg/ml of FL in MeCN), and each was made up to 500 μl with MeCN. The mixture was centrifuged for 10 min at 3000 rpm. A 20 μl aliquot of the supernatant fluid was subjected to HPLC.

Pharmacokinetic Calculations Apparent plasma clearance (CL_{app}) and apparent distribution volume at the steady state ($V_{ss,app}$) were obtained[17] using the area under the plasma concentration *vs.* time curve (AUC) and the mean residence time (MRT), which were calculated by applying the trapezoidal rule with extrapolation to infinity.[13] The terminal elimination rate constant (λ) was determined by least-squares linear regression of the logarithm of plasma concentration *vs.* time profiles. The values are given as mean values of data with standard deviation (S.D.). Student's t test was used as the test of significance.

The pharmacokinetic parameters (CL_{real} and $V_{ss,real}$) in the interconversion moment analysis and conversion fractions were calculated using the respective drug doses, AUC, fundamental clearances and $V_{ss,app}$ values as follows.[11,14,15]

Real plasma clearance;

$$CL_{real,D}=CL_{10}+CL_{12} \tag{31}$$

$$CL_{real,M}=CL_{20}+CL_{21} \tag{32}$$

TABLE II. Statistical Parameters of the Calibration Curves[a] for the Assay in the Rat

Compound		Regression		Correlation coefficient
		Slope (A)	Intercept (B)	(γ^2)
CRA	Plasma	9.136	9.88×10^{-4}	0.999
	Bile	8.016	2.73×10^{-4}	0.998
	Urine	7.392	5.83×10^{-4}	0.999
CR	Plasma	8.858	6.60×10^{-4}	0.998
	Bile	7.575	4.26×10^{-4}	0.999
	Urine	7.436	4.37×10^{-4}	0.998

a) Y(peak area ratio) = $B+AX$(μmol/ml).

Real distribution volume at the steady state;

$$V_{ss,real,D}=(V_{ss,app,D}-Kd_2^1V_{ss,app,M})/(1-Kd_2^1Kd_1^2) \tag{33}$$

$$V_{ss,real,M}=(V_{ss,app,M}-Kd_1^2V_{ss,app,D})/(1-Kd_2^1Kd_1^2) \tag{34}$$

where $Kd_2^1=CL_{12}CL_{21}/(CL_{20}+CL_{21})^2$ and $Kd_1^2=CL_{12}CL_{21}/(CL_{10}+CL_{12})^2$

First-time conversion fraction of metabolite to drug;

$$f_d=(AUC_D^{M_{iv}}/dose^{M_{iv}})/(AUC_D^{D_{iv}}/dose^{D_{iv}})=CL_{21}/(CL_{20}+CL_{21}) \tag{35}$$

First-time conversion fraction of drug to metabolite;

$$f_m=(AUC_M^{D_{iv}}/dose^{D_{iv}})/(AUC_M^{M_{iv}}/dose^{M_{iv}})=CL_{12}/(CL_{10}+CL_{12}) \tag{36}$$

Computer Analysis The multi-line fitting program used was MULTI written in Basic[18] for an NEC PC-9801 personal computer. The least-squares algorithm used was the Simplex method at the preliminary fitting, and the converged values were further analyzed by the modified Marquardt method. C^{-2} was adopted as the weight of data points. The plasma concentration *vs.* time equations of CRA (D) and CR (M) are:

$$C_D^{D_{iv}}=\frac{dose^{D_{iv}}}{V_1}\left[\frac{(E_2-\alpha)(k_{32}-\alpha)-k_{23}k_{32}}{(\beta-\alpha)(\gamma-\alpha)}e^{-\alpha t}+\frac{(E_2-\beta)(k_{32}-\beta)-k_{23}k_{32}}{(\alpha-\beta)(\gamma-\beta)}e^{-\beta t}+\frac{(E_2-\gamma)(k_{32}-\gamma)-k_{23}k_{32}}{(\alpha-\gamma)(\beta-\gamma)}e^{-\gamma t}\right]$$
$$=dose^{D_{iv}}(P_1e^{-\alpha t}+P_2e^{-\beta t}+P_3e^{-\gamma t}),\ (\beta>\gamma,\text{ and }\alpha=k_{10}+k_{12}) \tag{37}$$

$$C_M^{D_{iv}}=\frac{dose^{D_{iv}}k_{12}}{V_2}\left[\frac{(k_{32}-\alpha)}{(\beta-\alpha)(\gamma-\alpha)}e^{-\alpha t}+\frac{(k_{32}-\beta)}{(\alpha-\beta)(\gamma-\beta)}e^{-\beta t}+\frac{(k_{32}-\gamma)}{(\alpha-\gamma)(\beta-\gamma)}e^{-\gamma t}\right] \tag{38}$$

$$C_M^{M_{iv}}=\frac{dose^{M_{iv}}}{V_2}\left[\frac{(k_{32}-\beta)}{(\gamma-\beta)}e^{-\beta t}+\frac{(k_{32}-\gamma)}{(\beta-\gamma)}e^{-\gamma t}\right]$$
$$=dose^{M_{iv}}(Q_1e^{-\beta t}+Q_2e^{-\gamma t}) \tag{39}$$

$$C_D^{M_{iv}}=\frac{dose^{M_{iv}}k_{21}}{V_1}\left[\frac{(k_{32}-\alpha)}{(\beta-\alpha)(\gamma-\alpha)}e^{-\alpha t}+\frac{(k_{32}-\beta)}{(\alpha-\beta)(\gamma-\beta)}e^{-\beta t}+\frac{(k_{32}-\gamma)}{(\alpha-\gamma)(\beta-\gamma)}e^{-\gamma t}\right] \tag{40}$$

$$C_D^{D_{pv}}=\frac{dose^{D_{pv}}k}{V_1}\times\left[\frac{F_{H1}((E_2-\alpha)(k_{32}-\alpha)-k_{23}k_{32})+(1-F_{H1})F_{H2}k_{21}(k_{32}-\alpha)}{(\beta-\alpha)(\gamma-\alpha)(k-\alpha)}e^{-\alpha t}+\frac{F_{H1}((E_2-\beta)(k_{32}-\beta)-k_{23}k_{32})+(1-F_{H1})F_{H2}k_{21}(k_{32}-\beta)}{(\alpha-\beta)(\gamma-\beta)(k-\beta)}e^{-\beta t}+\frac{F_{H1}((E_2-\gamma)(k_{32}-\gamma)-k_{23}k_{32})+(1-F_{H1})F_{H2}k_{21}(k_{32}-\gamma)}{(\alpha-\gamma)(\beta-\gamma)(k-\gamma)}e^{-\gamma t}+\frac{F_{H1}((E_2-k)(k_{32}-k)-k_{23}k_{32})+(1-F_{H1})F_{H2}k_{21}(k_{32}-k)}{(\alpha-k)(\beta-k)(\gamma-k)}e^{-kt}\right] \tag{41}$$

$$C_M^{D_{pv}}=\frac{dose^{D_{pv}}k}{V_2}\left[\frac{F_{H1}k_{12}(k_{32}-\alpha)}{(\beta-\alpha)(\gamma-\alpha)(k-\alpha)}e^{-\alpha t}+\frac{F_{H1}k_{12}(k_{32}-\beta)+(1-F_{H1})F_{H2}(\alpha-\beta)(k_{32}-\beta)}{(\alpha-\beta)(\gamma-\beta)(k-\beta)}e^{-\beta t}+\frac{F_{H1}k_{12}(k_{32}-\gamma)+(1-F_{H1})F_{H2}(\alpha-\gamma)(k_{32}-\gamma)}{(\alpha-\gamma)(\beta-\gamma)(k-\gamma)}e^{-\gamma t}+\frac{F_{H1}k_{12}(k_{32}-k)+(1-F_{H1})F_{H2}(\alpha-k)(k_{32}-k)}{(\alpha-k)(\beta-k)(\gamma-k)}e^{-kt}\right] \tag{42}$$

where α, β and γ represent the rate constants, P_1, P_2, P_3, Q_1 and Q_2 are coefficients and the distribution volumes of compartments #1 and #2 are given by $V_1=1/(P_1+P_2+P_3)$ and $V_2=1/(Q_1+Q_2)$, respectively. Pharmacokinetic parameters to be estimated are set as P(1), P(2)$\cdots$ in Eqs. 37—42.

Results and Discussion

Plasma Concentration *vs.* Time Profiles and Dispositions of CRA and CR in the Rat Semilogarithmic plots of the mean plasma concentrations of CRA and CR against time after bolus iv administrations of 0.03 mmol/kg doses of CRA-K or CR are indicated in Fig. 2, and those after pv administration of 0.03 mmol/kg dose of CRA-K in Fig. 3. In both figures, a major characteristic of the metabolite CR generated from CRA is the nearly parallel decline in the terminal CRA and CR concentration *vs.* time curves. Thus, CRA is found to be in enzymatic equilibrium with CR in rats. The pharmacokinetic parameters obtained by the moment method are summarized in Table III.

The terminal log-linear slope ($\lambda_M=0.908\,h^{-1}$) of elimination of CR generated from CRA-K is not significantly different ($p>0.05$) from λ_D and λ_M values after independent iv doses of CRA-K and CR, respectively. Similarly, the terminal slope ($\lambda_D=0.874\,h^{-1}$) of CRA generated from CR is not significantly different ($p>0.05$) from the λ_D and λ_M

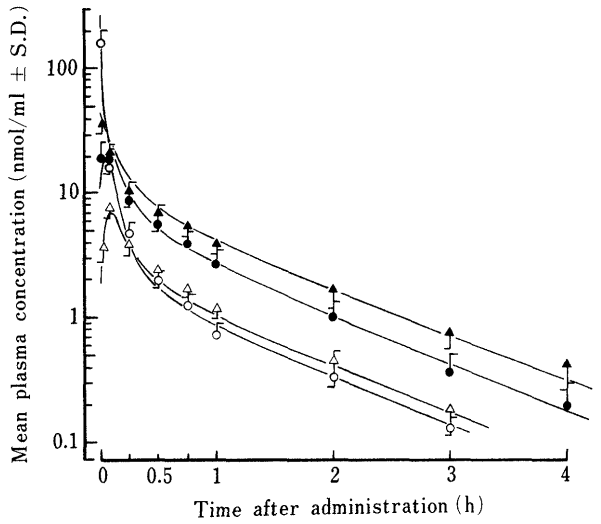

Fig. 2. Mean Plasma Concentration *vs.* Time Courses of the Drug and Its Metabolite Produced after Intravenous Administration of 0.03 mmol/kg Doses of Potassium Canrenoate CRA-K or Canrenone CR in Rats

○, CRA ($n=5$); ●, metabolite CR generated from CRA; ▲, CR ($n=5$); △, metabolite CRA generated from CR. Lines indicate the curves obtained by computer multi-line fitting.

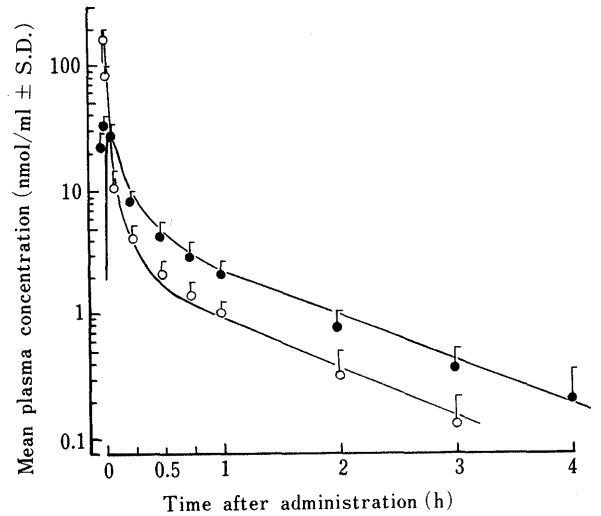

Fig. 3. Mean Plasma Concentration *vs.* Time Courses of the Drug and Its Metabolite Produced after Portal Vein Administration of 0.03 mmol/kg Dose of Potassium Canrenoate CRA-K in Rats

○, CRA ($n=5$); ●, metabolite CR generated from CRA. Lines indicate the curves obtained by computer multi-line fitting.

TABLE III. Pharmacokinetic Parameters[a] Calculated by the Moment Method after Intravenous (iv) and Portal Vein (pv) Administrations of 0.03 mmol/kg Doses of Potassium Canrenoate (CRA-K) or Canrenone (CR)

Drug		Administration site		
		iv	pv	
CRA-K				
λ_D	(h^{-1})	0.925±0.176	λ_D	0.917±0.141
$AUC_D^{D_{iv}}$	(nmol·h/ml)[b]	11.6 ±1.2	$AUC_D^{D_{pv}}$	8.77 ±0.19
$MRT_D^{D_{iv}}$	(h)	0.229±0.025	$MRT_D^{D_{pv}}$	0.341±0.086
$CL_{app,D}$	(l/h·kg)[c]	2.69 ±0.21		
$V_{ss,app,D}$	(l/kg)[d]	0.638±0.013		
$X_{bil,D}^{D_{iv}}$	(μmol/kg)[e]	0.203±0.079 (0.67%)		
$X_{ren,D}^{D_{iv}}$	(μmol/kg)	0.010±0.004 (0.04%)		
λ_M	(h^{-1})	0.908±0.161[f]	λ_M	0.866±0.155[h]
$AUC_M^{D_{iv}}$	(nmol·h/ml)	10.7 ±1.9	$AUC_M^{D_{pv}}$	9.77 ±1.37
$MRT_M^{D_{iv}}$	(h)	0.715±0.066	$MRT_M^{D_{pv}}$	0.784±0.141
$X_{bil,M}^{D_{iv}}$	(μmol/kg)	0.063±0.025 (0.21%)		
$X_{ren,M}^{D_{iv}}$	(μmol/kg)	0.003±0.001 (0.01%)		
CR				
λ_M	(h^{-1})	0.828±0.114		
$AUC_M^{M_{iv}}$	(nmol·h/ml)	15.4 ±2.5		
$MRT_M^{M_{iv}}$	(h)	0.881±0.110		
$CL_{app,M}$	(l/h·kg)	2.03 ±0.36		
$V_{ss,app,M}$	(l/kg)	1.70 ±0.18		
λ_D	(h^{-1})	0.874±0.229[g]		
$AUC_D^{M_{iv}}$	(nmol·h/ml)	4.30 ±0.28		
$MRT_D^{M_{iv}}$	(h)	0.895±0.135		

a) Each value indicates the mean±S.D. of five experiments. *b*) $AUC=\int_0^\infty Cdt+C_T/\lambda$ and $MRT=(\int_0^\infty tCdt+TC_T/\lambda+C_T/\lambda^2)/AUC$, where λ is the terminal elimination slope. *c*) Apparent plasma clearance: $CL_{app}=dose_{iv}/AUC$. *d*) Apparent distribution volume at the steady state: $V_{ss,app}=CL_{app}\cdot MRT$. *e*) X_{bil} and X_{ren} are cumulative amounts of drug or metabolite excreted into bile and urine (0—6 h), respectively. Percent of drug dose excreted into bile and urine is parenthesized. *f*, *g*) Not significantly different ($p>0.05$) from λ_D and λ_M after iv dosing of CRA-K and CR, respectively. *h*) Not significantly different ($p>0.05$) from both λ_D after iv and pv dosing of CRA-K.

TABLE IV. Pharmacokinetic Parameters and Available Fractions Characterizing the Reversible Disposition of CRA and CR in the Rat

Parameter and available fraction[a]	CRA (D)	CR (M)
CL_{10} (l/h·kg)	1.06	
CL_{12} (l/h·kg)	2.42	
CL_{20} (l/h·kg)	1.65	
CL_{21} (l/h·kg)	0.973	
CL_{real} (l/h·kg)	3.48	2.62
$V_{ss,real}$ (l/kg)	0.061	1.68
f_d	0.37	
f_m	0.69	
F_D	0.76	
F_M	0.91	
F	0.84	
F_{H1}	0.69	
F_{H2}	0.49	

a) See text for definition of symbols.

values after independent iv doses of CRA-K and CR. The plasma clearance is proportional to the elimination rate constant of the drug at constant volume of distribution. Therefore, it may be concluded that all clearance terms in the reversible CRA–CR system remain constant between treatments as defined in Eq. 5.

After iv administration of CRA-K, the biliary and urinary free fractions recovered within 6 h were 0.67% and 0.04%, and its metabolite CR collected in bile and urine were only 0.21% and 0.01% of the drug dose, respectively.

The parameters unique to the reversible drug–metabolite system, including the four fundamental clearances of reversible and irreversible elimination, real plasma clearances and real distribution volumes at the steady state, are indicated in Table IV. The real plasma clearance of CR, $CL_{real,M}$ is less than that of CRA ($CL_{real,D}$) at 2.62 l/h per kg. Nevertheless, the irreversible clearance process of metabolite CL_{20} is about 1.5 times larger than that of CRA (CL_{10}) at 1.65 l/h per kg. The metabolic process CL_{12} operating on CR is 2 times or more larger than the back-conversion process CL_{21} at 2.42 l/h per kg. The real distribution volume at the steady state of CRA, $V_{ss,real,D}$ is about one-tenth less than its apparent distribution volume at the steady state ($V_{ss,app,D}$) at 0.061 l/h per kg. The first-time conversion fraction of CRA to CR, f_m, is about 2 times larger than that of CR to CRA, f_d.

Estimation of the Available Fraction The available fractions calculated mathematically using Eqs. 28—30 are indicated in Table IV. The systemic available fraction of CRA, F_D, is 0.76, and the total available fraction as the sum of CRA and generated CR, F, is 0.84. The ratio, F_{H2}/f_m, being given less than unity, the AUC_M ratio of metabolite F_M cited above in Eq. 29 is appreciably less than unity at 0.91.

Figure 4 illustrates the relationships between the ratios of AUC at various values of F_{H1} and F_{H2}. The experimental result in the rat reversible CRA–CR system is plotted in the left-lower zone of Fig. 4. Thus, it may be considered that the application of CRA-K as a prodrug is useful in parenteral dosage form in order to avoid the sequential hepatic first-pass biotransformation of the generated active metabolite CR.

Simultaneous Computer Multi-Line Fitting of Plasma Concentration *vs.* Time Date The physiological or real volume of distribution at the steady state ($V_{ss,real}$) of the drug would be represented by the sum of the actual central and peripheral spaces of the drug. When the exponential Eqs. 37 and 39 are applied to each plot of the mean plasma concentration against time after independent iv doses of

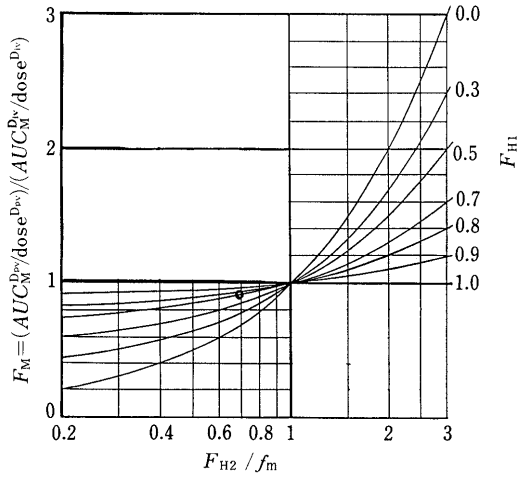

Fig. 4. Relationship among the Ratios of AUC Obtained from Intravenous and Intraportal Drug Administrations and the Available Fractions of Drug Dose

Equation 29 in the text was used to draw the curves. (○) indicates the point obtained from the reversible CRA–CR system in rats.

TABLE V. Pharmacokinetic Parameters[a] Obtained from the Plasma Concentration–Time Curve Fittings

Parameter	Initial value[b]	Simultaneous multi-line fitting	
	$C_D^{D_{iv}}$, $C_M^{M_{iv}}$	$C_D^{D_{iv}}$, $C_M^{D_{iv}}$, $C_M^{M_{iv}}$, $C_D^{M_{iv}}$	$C_D^{D_{iv}}$, $C_M^{D_{iv}}$, $C_M^{M_{iv}}$, $C_D^{M_{iv}}$, $C_D^{D_{pv}}$, $C_M^{D_{pv}}$
P_1 (kg/l)	9.45±3.78		
α (h^{-1})	51.7±22.6	37.5±7.6	36.0±2.1
Q_1 (kg/l)	1.04±0.18		
P_2 (kg/l)	0.846±0.458		
β (h^{-1})	8.09±1.92	8.44±2.58	9.74±1.94
Q_2 (kg/l)	0.329±0.044		
P_3 (kg/l)	0.0597±8.53×10^{-3}		
γ (h^{-1})	0.860±0.056	0.949±0.059	0.918±0.045
V_1 (1/kg)[c]	0.096	0.085±0.018	0.119±6.4×10^{-3}
V_2 (1/kg)	0.725	0.722±0.143	0.604±0.101
k_{10} (h^{-1})[d]	11.0	14.3±7.3	11.6±6.2
k_{12} (h^{-1})	25.2	23.1±5.2	24.4±5.0
k_{20} (h^{-1})	2.28	2.21±1.15	2.87±1.26
k_{21} (h^{-1})	1.34	0.996±0.276	1.53±0.34
k_{32} (h^{-1})[e]	2.59	3.09±0.91	2.65±0.58
k (h^{-1})[f]	14		18.4±13.8
F_{H1}[g]	0.69		0.68±0.62
F_{H2}	0.49		0.41±0.50
SS[h]	0.289	2.14	3.50
AIC[i]	−6.80	48.9	96.1

a) Converged values are given with standard deviation. *b*) $C_D^{D_{iv}}=dose^{D_{iv}}(P_1e^{-\alpha t}+P_2e^{-\beta t}+P_3e^{-\gamma t})$ and $C_M^{M_{iv}}=dose^{M_{iv}}(Q_1e^{-\beta t}+Q_2e^{-\gamma t})$. *c*) $V_1=1/(P_1+P_2+P_3)$ and $V_2=1/(Q_1+Q_2)$. *d*) $k_{10}=CL_{10}/V_1$, $k_{12}=CL_{12}/V_1$, $k_{20}=CL_{20}/V_2$ and $k_{21}=CL_{21}/V_2$. *e*) k_{32} is obtained from Eq. 20. *f*) $k=1/F_{H1}(MRT_D^{P_{iv}}-MRT_D^{D_{iv}})$. *g*) F_{H1} and F_{H2} are obtained by solving the simultaneous Eqs. 28 and 29. *h*) Residual sum of squares. $(C_i)^{-2}$ was adopted as the weight of data, where C_i is the value of the i-th point. *i*) An information criterion proposed by Akaike.[19]

CRA-K and CR, the distribution volume V_1 in the central compartment of CRA is obtained as 0.0961/kg, and V_2 of CR as 0.7251/kg as indicated in Table V. The V_1 value is almost close to $V_{ss,real,D}$ of CRA. On the other hand, the V_2 value is about one half of $V_{ss,real,M}$ of CR. Thus, the linear interconversion model indicated in Fig. 1 may be applicable, where CRA is treated by a one-compartment model and CR by a two-compartment model. In order to estimate the pharmacokinetic parameters by computer calculation, simultaneous multi-line fitting[9] of plasma concentration *vs.* time equations was carried out using the iterative nonlinear least-squares regression program, MULTI.[18]

The multi-line fitting of plasma concentration *vs.* time equations of C_D^{Div}, C_M^{Div}, C_M^{Miv} and C_D^{Miv} cited above in Eqs. 37—40 was tested. Then, using the converged values obtained as initial values, a similar fitting was made to the plasma concentration *vs.* time equations of C_D^{Div}, C_M^{Div}, C_M^{Miv}, C_D^{Miv}, C_D^{Dpv} and C_M^{Dpv} in Eqs. 37—42. The converged pharmacokinetic parameters are summarized in Table V, resulting in a successful agreement. The fitting curves are indicated in Figs. 2 and 3. The values of F_{H1} and F_{H2} were satisfactory at 0.68 and 0.41 in comparison with the values listed in Table IV.

Conclusion

A linear interconversion model incorporating a hepatic first-pass biotransformation was employed in order to assess the availabilities of CRA and its active metabolite CR in rats.

1) Biotransformation of CRA to CR is reversible, and the terminal slopes of the plasma concentration *vs.* time profile are nearly parallel. The first-time conversion fraction of CRA to CR, f_m, was obtained as 0.69.

2) In consequence of hepatic first-pass metabolism after pv administration of CRA-K, the values of F_{H1} and F_{H2} were obtained as 0.69 and 0.49, respectively. As the ratio, F_{H2}/f_m becomes less than unity, the AUC ratio of the metabolite, $F_M=(AUC_M^{Dpv}/\text{dose}^{Dpv})/(AUC_M^{Div}/\text{dose}^{Div})$ is appreciably less than unity.

3) The distribution volume V_1 of CRA is almost close to its $V_{ss,real,D}$. Therefore, the relationship $\alpha=k_{10}+k_{12}$ exists for the first-order rate constants of CRA, and the linear plasma concentration *vs.* time equation C_M^{Miv} of CR after iv administration is biexponential. The application of the multi-line fitting technique with the plasma concentration *vs.* time equations of CRA and its metabolite CR in an interconversion model (Fig. 1) seems to be useful to estimate the pharmacokinetic parameters.

Appendix

Symmetrical Linear Interconversion Model Analysis for iv Administered CRA and CR In Fig. 2, the terminal semilogarithmic slopes of mean plasma concentration against time for the drug and its generated metabolite after iv administration of CRA or CR resemble each other. Therefore, a symmetrical linear interconversion model[9b] is a possibility, as indicated in Fig. 5, where C_D, C_M, C_3 and C_4 are the drug concentrations and V_i ($i=1$ to 4) are the distribution volumes in the central (#1 and #2) and peripheral (#3 and #4) compartments, respectively.

The plasma concentration *vs.* time equations of CRA(D) and CR(M) in this model are as follows:

$$C_D^{Div}=\frac{\text{dose}^{Div}}{V_1}\left[\frac{(k_{31}-\alpha)[(E_2-\alpha)(k_{42}-\alpha)-k_{24}k_{42}]}{(\beta-\alpha)(\gamma-\alpha)(\delta-\alpha)}e^{-\alpha t}\right.$$
$$+\frac{(k_{31}-\beta)[(E_2-\beta)(k_{42}-\beta)-k_{24}k_{42}]}{(\alpha-\beta)(\gamma-\beta)(\delta-\beta)}e^{-\beta t}$$
$$+\frac{(k_{31}-\gamma)[(E_2-\gamma)(k_{42}-\gamma)-k_{24}k_{42}]}{(\alpha-\gamma)(\beta-\gamma)(\delta-\gamma)}e^{-\gamma t}$$
$$\left.+\frac{(k_{31}-\delta)[(E_2-\delta)(k_{42}-\delta)-k_{24}k_{42}]}{(\alpha-\delta)(\beta-\delta)(\gamma-\delta)}e^{-\delta t}\right]$$
$$=\text{dose}^{Div}(I_1e^{-\alpha t}+I_2e^{-\beta t}+I_3e^{-\gamma t}+I_4e^{-\delta t}),\qquad(\alpha>\gamma>\beta>\delta) \tag{43}$$

$$C_M^{Div}=\frac{\text{dose}^{Div}k_{12}}{V_2}\left[\frac{(k_{31}-\alpha)(k_{42}-\alpha)}{(\beta-\alpha)(\gamma-\alpha)(\delta-\alpha)}e^{-\alpha t}+\frac{(k_{31}-\beta)(k_{42}-\beta)}{(\alpha-\beta)(\gamma-\beta)(\delta-\beta)}e^{-\beta t}\right.$$
$$\left.+\frac{(k_{31}-\gamma)(k_{42}-\gamma)}{(\alpha-\gamma)(\beta-\gamma)(\delta-\gamma)}e^{-\gamma t}+\frac{(k_{31}-\delta)(k_{42}-\delta)}{(\alpha-\delta)(\beta-\delta)(\gamma-\delta)}e^{-\delta t}\right] \tag{44}$$

$$C_M^{Miv}=\frac{\text{dose}^{Miv}}{V_2}\left[\frac{(k_{42}-\alpha)[(E_1-\alpha)(k_{31}-\alpha)-k_{13}k_{31}]}{(\beta-\alpha)(\gamma-\alpha)(\delta-\alpha)}e^{-\alpha t}\right.$$
$$+\frac{(k_{42}-\beta)[(E_1-\beta)(k_{31}-\beta)-k_{13}k_{31}]}{(\alpha-\beta)(\gamma-\beta)(\delta-\beta)}e^{-\beta t}$$
$$+\frac{(k_{42}-\gamma)[(E_1-\gamma)(k_{31}-\gamma)-k_{13}k_{31}]}{(\alpha-\gamma)(\beta-\gamma)(\delta-\gamma)}e^{-\gamma t}$$
$$\left.+\frac{(k_{42}-\delta)[(E_1-\delta)(k_{31}-\delta)-k_{13}k_{31}]}{(\alpha-\delta)(\beta-\delta)(\gamma-\delta)}e^{-\delta t}\right]$$
$$=\text{dose}^{Miv}(J_1e^{-\alpha t}+J_2e^{-\beta t}+J_3e^{-\gamma t}+J_4e^{-\delta t}) \tag{45}$$

$$C_D^{Miv}=\frac{\text{dose}^{Miv}k_{21}}{V_1}\left[\frac{(k_{31}-\alpha)(k_{42}-\alpha)}{(\beta-\alpha)(\gamma-\alpha)(\delta-\alpha)}e^{-\alpha t}+\frac{(k_{31}-\beta)(k_{42}-\beta)}{(\alpha-\beta)(\gamma-\beta)(\delta-\beta)}e^{-\beta t}\right.$$
$$\left.+\frac{(k_{31}-\gamma)(k_{42}-\gamma)}{(\alpha-\gamma)(\beta-\gamma)(\delta-\gamma)}e^{-\gamma t}+\frac{(k_{31}-\delta)(k_{42}-\delta)}{(\alpha-\delta)(\beta-\delta)(\gamma-\delta)}e^{-\delta t}\right] \tag{46}$$

where α, β, γ and δ represent the individual rate constants, I_i ($i=1$ to 4) and J_j ($j=1$ to 4) are coefficients, and the following relationships hold:

$$E_1=k_{10}+k_{12}+k_{13},\quad E_2=k_{20}+k_{21}+k_{24} \tag{47}$$

$$\left.\begin{aligned}&E_1+k_{31}=\alpha+\beta,\quad E_2+k_{42}=\gamma+\delta\\&(E_1+k_{31})(E_2+k_{42})=(\alpha+\beta)(\gamma+\delta)\end{aligned}\right\} \tag{48}$$

$$k_{31}k_{42}=\alpha\beta\gamma\delta/(k_{10}k_{20}+k_{10}k_{21}+k_{12}k_{20}) \tag{49}$$

$$(k_{10}+k_{12})k_{31}+(k_{20}+k_{21})k_{42}=\alpha\beta+\gamma\delta+k_{12}k_{21} \tag{50}$$

$$[(\gamma+\delta)(k_{10}+k_{12})-k_{12}k_{21}]k_{31}$$
$$+[(\alpha+\beta)(k_{20}+k_{21})-k_{12}k_{21}]k_{42}=\alpha\beta(\gamma+\delta)+\gamma\delta(\alpha+\beta) \tag{51}$$

$$V_1=1/(I_1+I_2+I_3+I_4),\quad V_2=1/(J_1+J_2+J_3+J_4) \tag{52}$$

The computer multi-line fitting of C_D^{Div}, C_M^{Div}, C_M^{Miv} and C_D^{Miv} indicated in Eqs. 43—46 was tested. The converged pharmacokinetic parameters are listed in Table VI, and Akaike's information criterion (AIC)[19] was obtained as 55.7. This value is larger than 48.9 in Table V obtained from the multi-line fitting of the linear interconversion model where CRA is treated by a one-compartment model and CR by a two-compartment

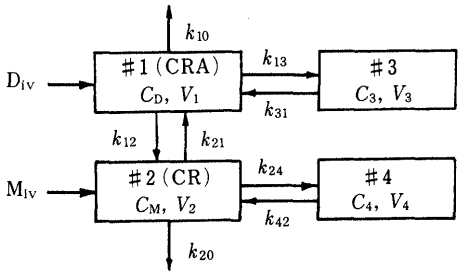

Fig. 5. Symmetrical Interconversion Model for CRA–CR System

See the text for details.

TABLE VI. Pharmacokinetic Parameters[a] Obtained from the Symmetrical Linear Interconversion Model Analysis

Parameter	Initial value	Multi-line fitting
	$C_D^{D_{iv}b)}$, $C_M^{M_{iv}c)}$	$C_D^{D_{iv}}$, $C_M^{D_{iv}}$, $C_M^{M_{iv}}$, $C_D^{M_{iv}}$
I_1 (kg/l)	8.42 ± 4.19	
J_1 (kg/l)	1.01 ± 0.58	
α $(h^{-1})^{d)}$	51.4 ± 31.2	53.9 ± 20.8
I_2 (kg/l)	0.0731 ± 0.312	
J_2 (kg/l)	0.196 ± 0.607	
β (h^{-1})	3.29 ± 2.93	3.90 ± 0.74
I_3 (kg/l)	0.455 ± 0.266	
J_3 (kg/l)	0.525 ± 0.615	
γ (h^{-1})	5.51 ± 1.69	6.19 ± 1.26
I_4 (kg/l)	0.0403 ± 0.0226	
J_4 (kg/l)	0.239 ± 0.141	
δ (h^{-1})	0.736 ± 0.175	0.762 ± 0.087
V_1 $(1/kg)^{e)}$	0.111	0.113 ± 0.013
V_2 (1/kg)	0.508	0.767 ± 0.253
k_{10} $(h^{-1})^{f)}$	9.55	11.8 ± 2.78
k_{12} (h^{-1})	21.8	28.0 ± 11.7
k_{20} (h^{-1})	3.24	2.10 ± 0.95
k_{21} (h^{-1})	1.92	1.74 ± 1.60
k_{31} $(h^{-1})^{g)}$	6.64	6.43 ± 2.88
k_{42} (h^{-1})	1.03	1.48 ± 0.39
$SS^{h)}$	0.184	2.35
$AIC^{i)}$	-6.51	55.7

a) Converged values are given with standard deviation. *b*) $C_D^{D_{iv}} = \text{dose}^{D_{iv}} \times (I_1 e^{-\alpha t} + I_2 e^{-\beta t} + I_3 e^{-\gamma t} + I_4 e^{-\delta t})$ at 0.03 mmol/kg dose of CRA-K. *c*) $C_M^{M_{iv}} = \text{dose}^{M_{iv}} (J_1 e^{-\alpha t} + J_2 e^{-\beta t} + J_3 e^{-\gamma t} + J_4 e^{-\delta t})$ at 0.03 mmol/kg dose of CR. *d*) $\alpha + \beta > \gamma + \delta$ because of $MRT_D^{D_{iv}} < MRT_M^{M_{iv}}$. *e*) $V_1 = 1/(I_1 + I_2 + I_3 + I_4)$ and $V_2 = 1/(J_1 + J_2 + J_3 + J_4)$. *f*) $k_{10} = CL_{10}/V_1$, $k_{12} = CL_{12}/V_1$, $k_{20} = CL_{20}/V_2$ and $k_{21} = CL_{21}/V_2$. *g*) k_{31} and k_{42} are obtained by solving the simultaneous Eqs. 50 and 51. *h*) Residual sum of squares at the weight of data of C^{-2}. *i*) An information criterion proposed by Akaike.

model.

Akaike[20] proposed the minimum *AIC* estimation to select the best model from several possible models. This estimation also selects the model with the smaller number of parameters according to the 'principle of parsimony.' It may be concluded that symmetrical linear interconverstion model analysis as shown in Fig. 5 for the CRA–CR system should be rejected in the present case.

References

1) A. Gochman and C. L. Gantt, *J. Pharmacol. Exp. Ther.*, **135**, 312 (1962).
2) E. Gerhards and R. Engelhardt, *Arzneim.-Forsch.*, **13**, 972 (1963).
3) L. Zicha, F. Weist, F. Scheiffarth and E. Schmidt, *Arzneim.-Forsch.*, **14**, 699 (1964).
4) H. Wagner, F. Weist and L. Zicha, *Arzneim.-Forsch.*, **17**, 415 (1967).
5) *a*) W. Sadée, S. Riegelman and S. C. Jones, J. *Pharm. Sci.*, **61**, 1129 (1972); *b*) W. Sadée, M. Dagcioglu and R. Schröder, *J. Pharmacol. Exp. Ther.*, **185**, 686 (1973).
6) E. R. Garrett and C. M. Won, *J. Pharm. Sci.*, **60**, 1801 (1971).
7) *a*) A. Karim, R. E. Ranney and H. I. Maiback, *J. Pharm. Sci.*, **60**, 708 (1971); *b*) A. Karim, J. Zagarella, J. Hribar and M. Dooley, *Clin. Pharmacol. Ther.*, **19**, 158 (1976).
8) K. Kojima, K. Yamamoto, H. Fujioka and H. Kaneko, *J. Pharmacobio-Dyn.*, **8**, 161 (1985).
9) *a*) S. Inui, T. Otawa, H. Nakae and S. Asada, *Chem. Pharm. Bull.*, **36**, 1922 (1988); *b*) S. Nagamine (née Inui), H. Nakae and S. Asada, *Yakugaku Zasshi*, **108**, 1072 (1988).
10) K. S. Pang and J. R. Gillette, *J. Pharmacokinet. Biopharm.*, **7**, 275 (1979).
11) W. F. Ebling and W. J. Jusko, *J. Pharmacokinet. Biopharm.*, **14**, 557 (1986).
12) D. P. Vaughan and A. Trainor, *J. Pharmacokinet. Biopharm.*, **3**, 203 (1975).
13) K. Yamaoka, T. Nakagawa and T. Uno, *J. Pharmacokinet. Biopharm.*, **6**, 547 (1978).
14) S. Nagamine, T. Otawa, H. Nakae and S. Asada, *Chem. Pharm. Bull.*, **36**, 4612 (1988).
15) S. Asada, S. Nagamine and H. Nakae, *Chem. Pharm. Bull.*, **37**, 760 (1989).
16) J. A. Cella, E. A. Brown and R. R. Burtner, *J. Org. Chem.*, **24**, 743 (1959).
17) L. Z. Benet and R. L. Galeazzi, *J. Pharm. Sci.*, **68**, 1071 (1979).
18) K. Yamaoka, T. Nakagawa, H. Tanaka, M. Yasuhara, K. Okumura and R. Hori, *J. Pharmacobio-Dyn.*, **8**, 246 (1985).
19) K. Yamaoka, T. Nakagawa and T. Uno, *J. Pharmacokinet. Biopharm.*, **6**, 165 (1978).
20) H. Akaike, *IEEE Trans. Automat. Control.*, **19**, 713 (1973).